Vasopressin depolymerizes apical F-actin in rat inner medullary collecting duct

HEROLD SIMON, YANG GAO, NICHOLAS FRANKI, AND RICHARD M. HAYS
Division of Nephrology, Department of Medicine,
Albert Einstein College of Medicine, Bronx, New York 10461

Simon, Herold, Yang Gao, Nicholas Franki, and Richard M. Hays. Vasopressin depolymerizes apical F-actin in rat inner medullary collecting duct. *Am. J. Physiol.* 265 (*Cell Physiol.* 34): C757-C762, 1993.—In amphibian bladder, arginine vasopressin (AVP) depolymerizes F-actin in the apical region of the granular cell, promoting fusion of water channel-carrying vesicles with the apical membrane. We now report the effect of AVP on F-actin in the mid- and terminal segments of rat inner medullary collecting duct ($IMCD_2$ and $IMCD_3$). In $IMCD_3$, 5 min of stimulation by 2.5-250 nM AVP significantly depolymerized F-actin by 13-24% in whole cell assays employing the rhodamine-phalloidin binding technique. The $IMCD_2$ was more sensitive, responding to subnanomolar (0.25 nM) AVP with $6 \pm 2\%$ depolymerization. Depolymerization occurred as early as 2 min after 2.5 and 25 nM but not 250 nM AVP. 8-Bromoadenosine 3',5'-cyclic monophosphate depolymerized F-actin in $IMCD_3$ at both 2 and 5 min. Immunogold labeling of the apical actin pool in $IMCD_3$ principal cells was reduced by $26 \pm 5\%$ ($P < 0.05$) by 2.5 nM AVP; the lateral and basal pools showed no significant changes. Capillary endothelial, thin limb of Henle, and intercalated cells showed no changes in immunogold labeling after AVP. Thus reorganization of the apical actin network by AVP is a consistent finding in both mammalian and amphibian target cells.

cytoskeleton; antidiuretic hormone; water channels

STUDIES in the amphibian urinary bladder (4-6, 8, 10, 12) have shown that arginine vasopressin (AVP) rapidly depolymerizes F-actin and that the depolymerization takes place in the apical region of the granular cell where aggrephores are positioned. These studies suggest that cytoskeletal actin, along with other filaments, provides a network that holds the aggrephores in place in the unstimulated cell and acts as a barrier to fusion. The network would then break down in the presence of AVP, permitting aggrephores to move and fuse with the apical membrane.

We now present studies showing that AVP and 8-bromoadenosine 3',5'-cyclic monophosphate (8-BrcAMP) depolymerize F-actin in the two distal segments of the rat inner medullary collecting duct (IMCD) and that AVP, as in the amphibian bladder, acts on the apical actin pool. In comparing the response of the two segments of the IMCD, we found that the midsegment ($IMCD_2$) was more sensitive than the terminal segment ($IMCD_3$) to the depolymerizing action of AVP.

METHODS

Tissue preparation. Sprague-Dawley rats (Charles River Laboratories, Kingston NY) weighing 250-300 g were fed standard rat chow and allowed to drink tap water ad libitum. They were anesthetized with an intraperitoneal injection of pentobarbital sodium (5 μg/100 g body wt; Anthony Products, Arcadia, CA). Both kidneys were quickly removed and placed in 30 ml of ice-cold buffer composed of (in mM) 118 NaCl, 25 $NaHCO_3$, 0.5 $CaCl_2$, 2.5 K_2HPO_4, 1.2 $MgSO_4$, 5.5 glucose, 5 creatinine, and 5 urea (285 mosmol/kgH_2O). This buffer was identical to that employed by Lankford et al. (14) except for a lower Ca^{2+} concentration in anticipation of the Ca^{2+} removal step. The kidney was sectioned coronally, and the papilla was exposed. Either the bottom half of the papilla containing the $IMCD_3$ or its upper half containing largely the $IMCD_2$ was dissected into fine sections of ~0.3-mm thickness with a razor blade. The sections were washed for an additional 10 min in the above buffer gassed with 95% O_2-5% CO_2 with a final pH of 7.4. The sections were then placed in 10 ml of gassed buffer in the presence of 0.1% collagenase (type V), 0.1% hyaluronidase (type III), and 0.1% bovine serum albumin (Sigma Chemical, St. Louis MO) for 30 min and then washed twice for successive 10-min periods in collagenase-free buffer. The total incubation time at this point was somewhat over 60 min, exceeding the time required to bring osmotic water flow in perfused tubules from antidiuretic rats to baseline values (14). Exposure to the collagenase and hyaluronidase resulted in the opening up of the sections (Fig. 1) so that they became easily penetrated by the outside buffer and by AVP and other agents used in the experiments.

After the preliminary incubations, individual sections were placed in separate tubes containing 5 ml of the above buffer at 37°C and incubated with AVP (Sigma) or 8-BrcAMP (Plenum Scientific, Hackensack NJ) for varying time periods. Tissues not exposed to AVP or 8-BrcAMP and incubated for identical time periods were used as controls. To remove Ca^{2+} from the buffer before fixation, 4 mM ethylene glycol-bis(β-aminoethyl ether)-*N,N,N',N'*-tetraacetic acid (EGTA) was added to each tube for the last minute of the incubation period.

Rhodamine-phalloidin binding assay. Fixation was carried out in 3.7% formaldehyde including 0.1% Triton X-100 in the isotonic buffer for 30 min. Triton X-100 was added to increase the rapidity of fixation (3). Sections were then further divided into many fine pieces, and the suspension of fine pieces was divided equally into three separate 1.5-ml Eppendorff tubes for triplicate determination. The procedure of Ding et al. (4) was then used to determine F-actin. Tissue pieces were washed in buffer containing 40 mM KH_2PO_4, 10 mM piperazine-*N,N'*-bis(2-ethanesulfonic acid), 5 mM EGTA, and 2 mg SO_4 (pH 6.8). The tubes were then centrifuged at 12,500 *g* for 2 min, the supernatant was removed, and the pellets were resuspended in buffer containing 0.3 μM of rhodamine-phalloidin (Molecular Probes, Portland OR), a saturating concentration, and 0.1% saponin and rotated in the dark for 60 min. After the staining step, the pellets were washed once with the saponin buffer and 600 μl of 100% methanol were placed in the tubes to extract the rhodamine. The tubes were rotated in the dark for 30 min, the methanol was pipetted into a cuvette, and fluorescence was read in a Perkin-Elmer model MPF-3L spectrofluorometer (Norwalk, CT). Each experimental point was determined in triplicate as noted above.

Protein content of the tissue pellets was determined by the Bradford method (Bio-Rad protein assay, Bio-Rad, Cambridge, MA), and fluorescence was expressed per microgram of protein. Means of control vs. AVP or 8-BrcAMP sections were compared by pair analysis using Student's *t* test.

0363-6143/93 $2.00

Immunogold labeling of actin. To localize the effect of AVP on actin in the principal cell, we used the quantitative immunogold method of Gao et al. (6), which had been employed in studies of the toad bladder. Briefly, $IMCD_3$ tissue pieces incubated as controls or stimulated by AVP using the same protocol as for the rhodamine-phalloidin binding assay were fixed after 5 min in 4% paraformaldehyde and 0.1% glutaraldehyde. After 1-h fixation, tissues were dehydrated and embedded in LR Gold (EM Sciences, Fort Washington PA). Thin sections of the polymerized block were stained with an affinity-purified mouse monoclonal antibody to chicken gizzard actin (Boehringer Mannheim, Indianapolis IN); the secondary antibody was goat anti-mouse immunoglobulin G coating the surface of 10-nm gold particles. Specificity of the primary antibody labeling of rat kidney actin was confirmed by Western blot showing a single band at 43 kDa. Principal cells of the terminal IMCD were viewed at random on the video monitor of a Jeol 1200 EX electron microscope at 80-kV accelerating voltage. Quantitative analyses were done in a blind fashion on coded samples by placing transparent films over the video monitor, tracing the apical cell outline with a pen, and placing a dot for each gold particle. Particle frequency (per μm^2) was determined for the cortical region to a depth of 0.5 μm below the apical membrane and separately for the microvilli. The areas of cortex and microvilli were determined with a Numonics Graphic Calculator (Lansdale PA). Statistical differences between paired control and AVP samples were again determined by Student's t test for paired data.

Microscopy. Representative light- and electron microscopic views of IMCD sections (Figs. 1 and 2) were obtained from thin sections of medulla fixed with 2% glutaraldehyde, embedded in Epon, and sectioned with a Reichert-Jung Ultracut E microtome. They were either viewed with the Jeol 1200 EX electron microscope or stained with toluidine blue and viewed with a Zeiss Axiophot light microscope. The laser-scanning confocal image (Fig. 2*A*) was obtained with a Bio-Rad MRC-600 scanning microscope on a formaldehyde-fixed section of rat medulla permeabilized by saponin and stained with rhodamine-phalloidin (5).

RESULTS

Morphology. As in the toad urinary bladder, F-actin is distributed along the periphery of the cells of the rat IMCD. Figure 2*A* shows the distribution of rhodamine-phalloidin-stained F-actin in an optical section of the IMCD obtained with the laser-scanning confocal microscope. The apical and lateral borders of the tubular cells are heavily labeled, and F-actin is present along the base as well. Figure 2, *B* and *C*, shows the course of F-actin and other filaments in the principal cell of the IMCD compared with an intercalated cell. In the principal cell, the filaments follow an unusual course, running down from the microvilli and then forming a network below the apical membrane. This pattern is similar to that of the AVP-sensitive granular cell of the toad urinary bladder (9, 16) and suggests that actin may form a submembranous barrier to vesicular fusion. In the intercalated cell as well as the proximal tubular cell (not shown), the actin filaments follow a more typical course for epithelia, running down the microvilli and continuing straight into the terminal web.

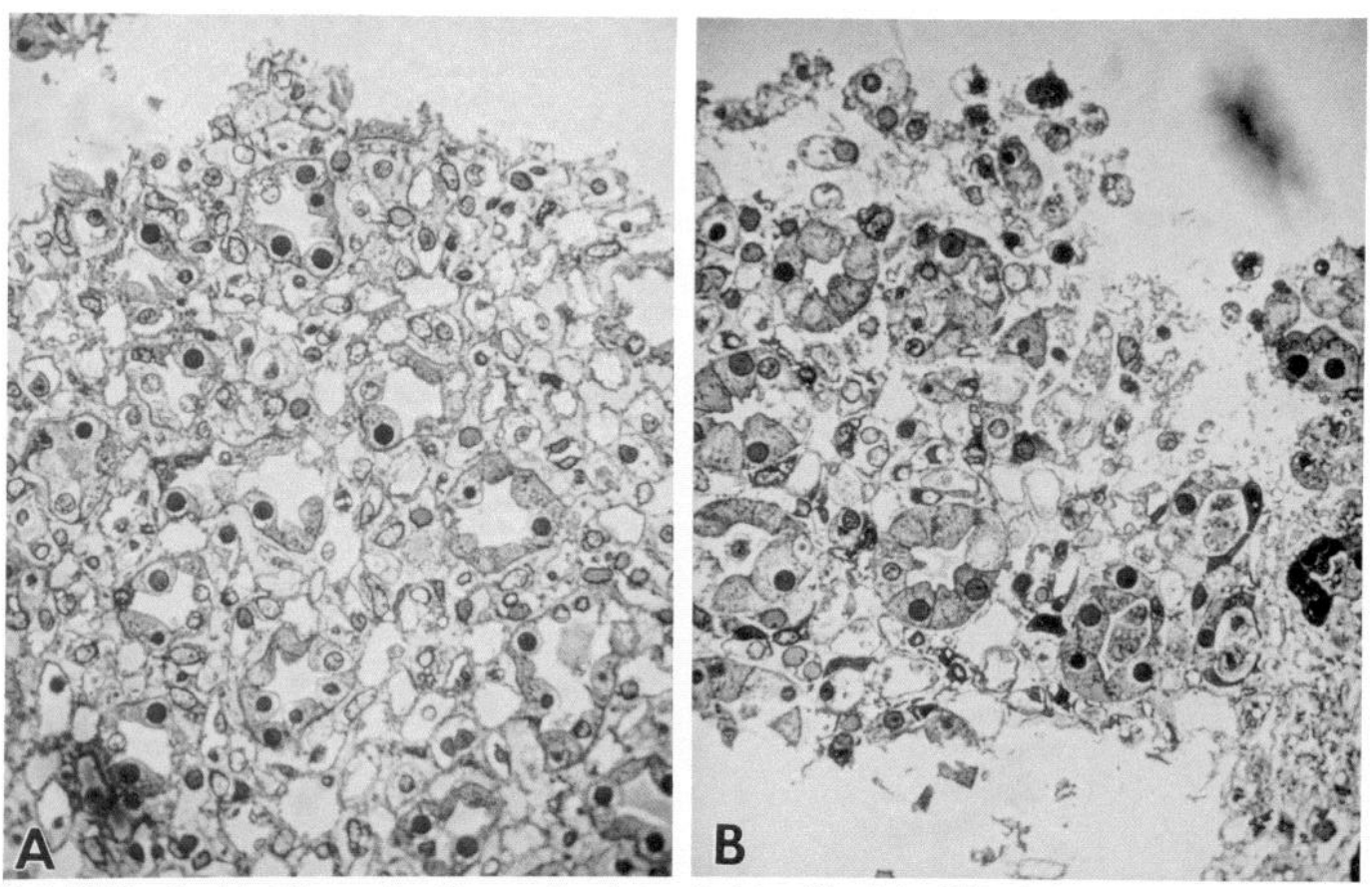

Fig. 1. Toluidine blue-stained Epon section of lower portion of rat papilla before (*A*) and after (*B*) incubation in collagenase-hyaluronidase-containing buffer. Opening up of tissue is seen in *B*. Magnification ×350.

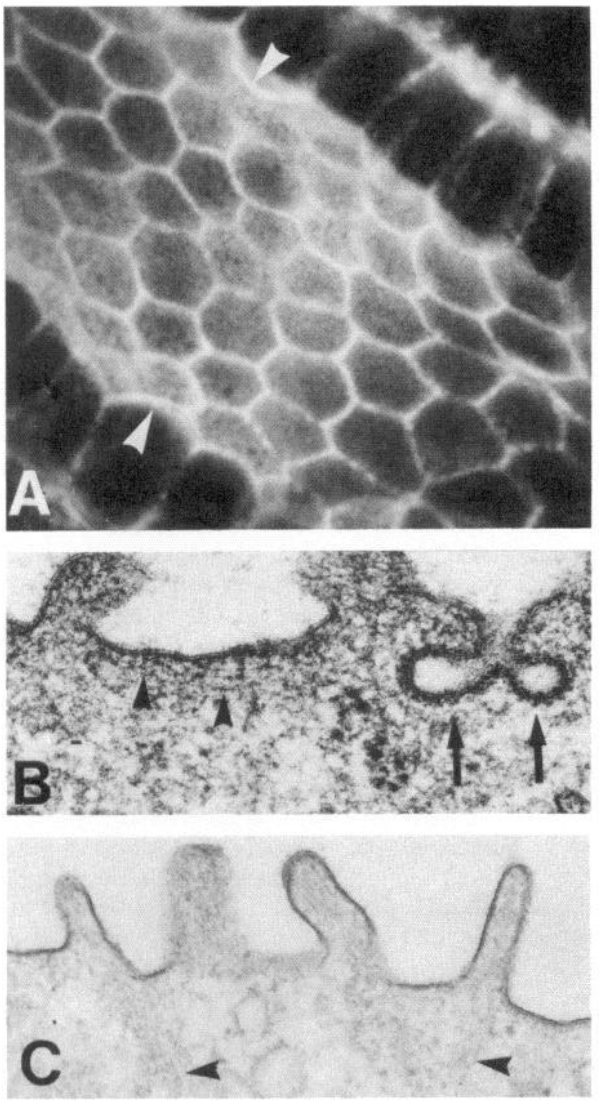

Fig. 2. *A*: scanning confocal view of an inner medullary collecting duct (IMCD) stained for F-actin with rhodamine-phalloidin. Epithelial cells along sides of tubule show actin along their apical borders (arrowheads) as well as along their lateral and basal borders. *B*: transmission electron-microscopic view of apical region of a principal cell fixed with glutaraldehyde-tannic acid. Filaments are seen running below apical membrane (arrowheads). *C*: intercalated cell, showing filaments running straight into terminal web (arrowheads). Magnification ×1,200 (*A*); ×54,000 (*B*); ×81,000 (*C*).

Table 1. *Effect of AVP on whole cell actin*

Segment	Time of AVP Incubation, min	*n*	AVP, nM	Fluorescence/μg protein		
				Control	AVP	Δ
$IMCD_3$	5	7	0.25	1.11±0.06	1.12±0.05	−0.01±0.03
		8	2.5	1.33±0.07	1.16±0.06	0.17±0.07*
		6	25	1.37±0.10	1.20±0.08	0.17±0.06*
		6	250	1.25±0.24	0.95±0.17	0.30±0.11*
$IMCD_3$	2	7	2.5	1.37±0.12	1.31±0.11	0.06±0.02*
		8	25	1.57±0.12	1.38±0.08	0.19±0.07*
		4	250	1.50±0.07	1.52±0.07	−0.02±0.04
$IMCD_2$	5	10	0.25	1.08±0.05	1.02±0.05	0.06±0.02*

Values are means ± SE; *n*, no. of rats. $IMCD_2$ and $IMCD_3$, mid- and terminal segments of inner medullary collecting duct, respectively. * $P < 0.05$ for control vs. arginine vasopressin (AVP; paired *t* test).

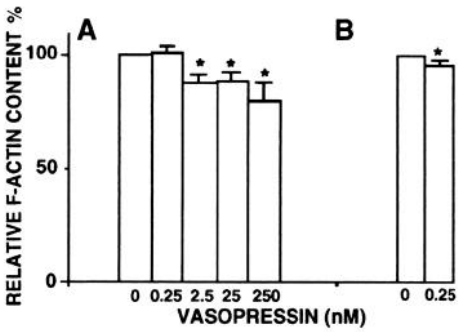

Fig. 3. Relative whole cell F-actin content of terminal segment of IMCD ($IMCD_3$; *A*) and midsegment of IMCD ($IMCD_2$; *B*) incubated for 5 min with arginine vasopressin (AVP) at concentrations shown. Bars, SE; * significantly different from control.

Effects of AVP and cAMP on whole cell F-actin. The results of these experiments are shown as relative changes (AVP or cAMP vs. control) in Figs. 3–5 and as fluorescence values in Table 1. Figure 3 shows the effect of 5 min of exposure to AVP on the relative F-actin content of the $IMCD_3$ (*A*) and $IMCD_2$ (*B*), compared with their respective paired controls. In the $IMCD_3$ a small and not significant decrease in F-actin was seen after 0.25 nM AVP; significant decreases from 12 to 20% were seen after 2.5–250 nM. To determine whether the $IMCD_2$ was more sensitive to AVP, we again determined the effect of 0.25 nM AVP on actin in this subsegment (Fig. 3*B*). We found a small (6 ± 2%) decrease in F-actin which was significant ($P = 0.05$, $n = 10$).

We were able to detect significant depolymerization (4–12%) as early as 2 min after stimulation by 2.5 and 25 nM AVP in the $IMCD_3$ (Fig. 4); 250 nM, a very high concentration, had no effect, however, in contrast to its effect at 5 min.

8-BrcAMP was effective in depolymerizing F-actin in the $IMCD_3$ after 2 and 5 min of stimulation (Fig. 5); the extent of depolymerization at both time points was 18%.

Immunogold labeling of actin. Figure 6 shows the distribution and frequency of gold particles in the apical region of $IMCD_3$ principal cells from three control rats (*A*, *C*, and *E*) and paired tissues from the same rats incubated for 5 min with 2.5 nM AVP (*B*, *D*, and *F*). The frequency of particles was determined for the cortical region to a depth of 0.5 μm below the apical membrane and separately for the microvilli. (It should be noted that some of the microvilli in the control and AVP-treated

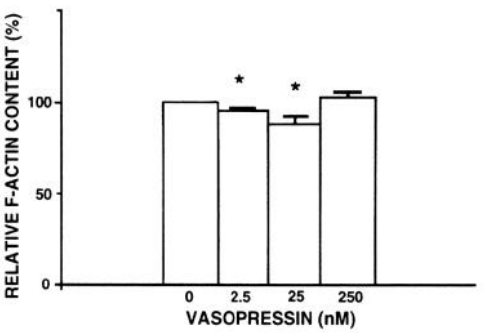

Fig. 4. Relative whole cell actin content of $IMCD_3$ incubated for 2 min with AVP.

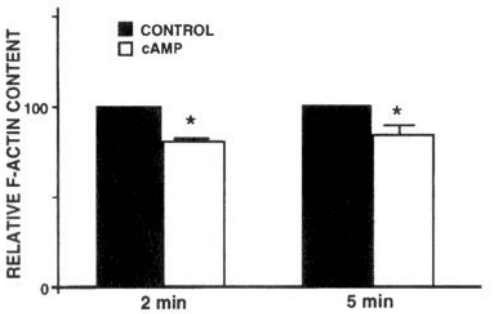

Fig. 5. Effect of 8-BrcAMP on $IMCD_3$ at 2 and 5 min.

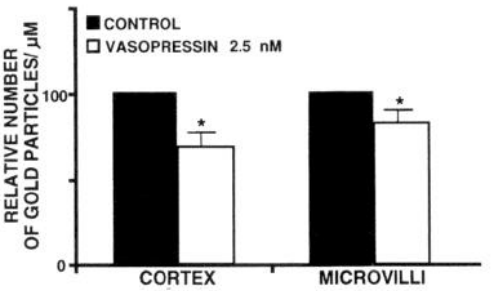

Fig. 7. Effect of 2.5 nM AVP on immunogold labeling of cortex and microvilli.

tissues are not discrete sharply defined structures but instead more continuous with the underlying cortex.) As noted in METHODS, the immunogold determinations were done without knowledge of experimental conditions. In a total of seven paired experiments, there was a significant decrease in particle frequency in both cortex and microvilli (Fig. 7). The decrease in cortical frequency (26%) was twice that determined for whole cell actin with the rhodamine-phalloidin method (13%), since the immunogold method focuses exclusively on the AVP-sensitive actin pool. The decrease in actin labeling of the microvilli in the $IMCD_3$ cells was not seen in our earlier study of the toad bladder (6) and will be considered in the DISCUSSION.

Because the principal cells are only a portion of the total cell population in the papilla, it was important to determine by the immunogold method whether the actin pools in capillary endothelial cells and thin limb of Henle cells responded to AVP. We also included the few intercalated cells that were present in the sections. We surveyed the above cells in paired sections taken from our original series of seven, using paired sections that had shown a decrease in apical actin labeling after 2.5 nM AVP. As in the apical study, this study was performed without knowledge of which of a given pair was control and which was AVP treated. In addition, we determined the effect of AVP on labeling of the lateral and basal domains of the principal cells themselves to determine whether these actin pools were AVP sensitive. The results are shown in Table 2. It should be noted that for the capillary and thin limb cells data for microvilli and cortex were pooled; separate analyses also showed no significant change for microvilli and cortex. We found that in no cell other than the principal cell was there a significant decrease in immunogold labeling. In the lateral and basal regions of the principal cell, there was again no significant change in immunogold labeling. Thus the apical region of the principal cell was the sole actin pool responding to AVP.

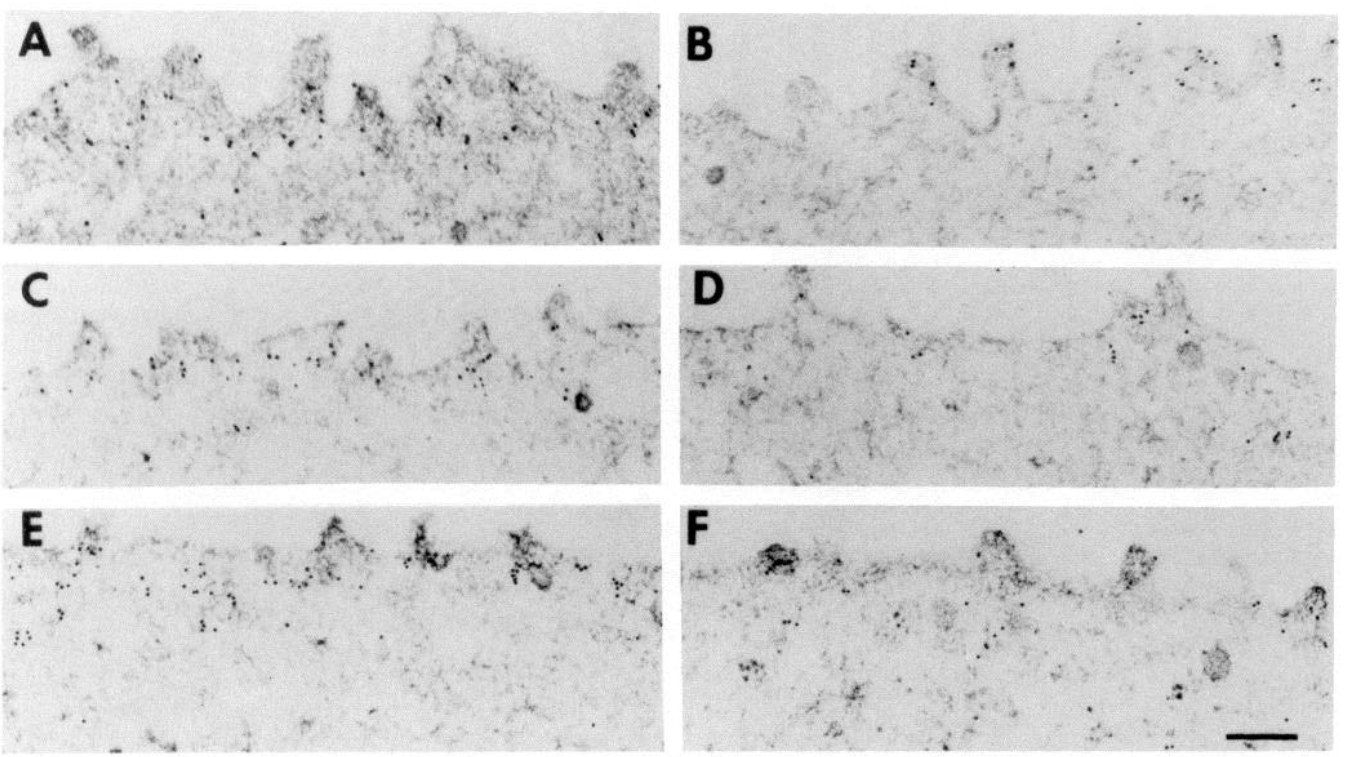

Fig. 6. Immunogold labeling of apical region of $IMCD_3$ principal cells. *A*, *C*, and *E*: controls; *B*, *D*, and *E*: paired sections after 5 min of 2.5 nM AVP. Bar = 0.2 μm.

Table 2. *Effect of AVP on immunogold labeling of rat papillary cells*

Cell	n	Particle Frequency/μm^2		
		Control	AVP	Δ
IMCD principal cell				
Apical cortex	7	31.5±5.4	21.7±2.9	9.8±3.8*
Apical microvilli	7	62.2±5.5	51.3±5.0	10.9±3.5*
Lateral cortex	4	14.0±2.3	13.9±3.8	0.1±3.6
Lateral folds	4	54.9±12.3	51.0±11.5	3.9±3.3
Basal cortex	7	13.6±2.4	10.5±1.4	3.1±1.8
Intercalated cell				
Apical cortex	3	31.3±11.5	30.1±10.3	1.2±1.6
Apical microvilli	3	56.5±25.5	51.1±18.2	5.4±7.4
Basal cortex	3	48.3±15.1	44.7±20.0	3.6±5.0
Capillary endothelial cell	4	14.1±2.3	12.4±4.2	1.7±2.7
Thin limb of Henle's loop	4	16.5±4.5	14.4±1.3	2.1±3.7

Values are means ± SE; *n*, no. of rats. * $P < 0.05$ for control vs. AVP (paired *t* test).

DISCUSSION

These studies show that in the rat IMCD, as in the amphibian urinary bladder, AVP depolymerizes F-actin. After 5 min of exposure to AVP, the F-actin content of intact $IMCD_3$ cells was reduced by 13% by 2.5 nM AVP and by as much as 24% by 250 nM of the hormone. The $IMCD_2$ was more sensitive to AVP, showing a small but significant (6 ± 2%) depolymerization by 0.25 nM AVP. We did not study the effect of an even lower AVP concentration. Although the effect of 0.25 nM AVP on whole cell actin was a small one, we would assume that the change in the apical actin pool itself would be higher, as it proved to be in the immunogold studies at 2.5 nM AVP. It should be kept in mind that only a small amount of F-actin may have to be depolymerized to free up the water channel-carrying vesicles, even less than measured in our studies. Also, actin depolymerization alone is probably not enough to promote vesicle fusion, which may require transport along microtubules and other cellular responses to AVP.

The difference in sensitivity of the depolymerization response of the $IMCD_2$ and $IMCD_3$ may reflect differences in both structure and function of the cells in these two segments. Most of the $IMCD_2$ and all of the $IMCD_3$ in the rat consist of a distinct cell type, the "IMCD cell," which differs in appearance from the principal cell of $IMCD_1$ (15). Freeze-fracture studies by Lacey (13) have shown a sharply decreased density of intramembranous particle clusters in the luminal plasma membranes of IMCD cells at the papillary tip in antidiuretic rats compared with cells at the base of the papilla. This suggests a reduced response to AVP in the very terminal part of $IMCD_3$, a portion of the collecting duct that was removed in studies of water movement across this segment (14, 17). Because the segments in our study included presumably less responsive cells in the terminal papilla, it is possible that this contributes to the reduced sensitivity. The cells in the $IMCD_2$, on the other hand, may well have had a more uniform and more easily detectable response.

At an earlier time point, 2 min, we were able to show depolymerization at 2.5 and 25 nM AVP but found no significant depolymerization at 250 nM, a very high concentration. Han et al. (7) have shown that relatively high concentrations of AVP produce a considerably lower water flow response in the isolated perfused rat IMCD than concentrations in the nanomolar range, and the failure to show actin depolymerization may reflect this paradoxical effect of AVP. By 5 min, however, even this high concentration had become effective in depolymerizing F-actin. Aside from this unresolved question of the time-dependent action of 250 nM AVP, we would conclude that AVP depolymerizes F-actin in the mammalian collecting duct as in the toad and frog urinary bladders.

Immunogold studies of the apical region of the principal cell showed a considerably higher percentage of depolymerization (26%) at 2.5 nM AVP than that seen in measurements of whole cell actin at this concentration of AVP (13%). This would be the expected result from studies looking directly at the AVP-responsive actin pool and is important in evaluating the relatively small changes we observed in whole cell actin. The microvilli shared in this response, unlike the microvilli in the toad bladder. From Fig. 6, it appears that the actin in the IMCD microvilli may be more continuous with the pool of actin in the cortical region than in the toad bladder and is depolymerized to some extent along with the cortical actin.

The depolymerizing effect of AVP on F-actin was limited to the apical actin pool of the IMCD principal cells, as shown by the immunogold measurements (Table 2). Capillary endothelial, loop of Henle, and intercalated cells did not show a decrease in immunogold labeling in the presence of AVP, and within the principal cells themselves, neither the lateral nor the basal actin pools were responsive to hormone. These findings support our interpretation of the rhodamine-phalloidin studies as reflecting changes in the apical actin pool of the principal cells.

Why the principal cells should respond to AVP and the other cells in the medulla show no response may simply be a matter of having or not having the proper AVP-initiated signaling system. The fact that, within the principal cell, only the apical F-actin pool is AVP sensitive is of some interest. There may be specific intermediates such as cAMP-dependent kinases that are only coupled to the apical actin pool. It is also possible that the F-actin in the lateral and basal pool is organized in such a way as to be nonresponsive. Certain actin-binding proteins, for example, may protect actin filaments from disassembly (18, 19).

An important question is the extent to which actin depolymerization is required for water flow to take place in the IMCD and the extent to which water flow can proceed without depolymerization. In considering this problem, it is useful to compare the sensitivity of the depolymerization response to AVP in toad bladder and IMCD in relation to the sensitivity of their water flow responses and in relation to the systems for water channel delivery. In the unstimulated toad bladder, aggrephores are positioned in a region 0.1–0.5 μm beneath the apical membrane (9). To fuse with the membrane, most if not all of the aggrephores may have to detach from and penetrate at least part of the subapical actin network. Under these circumstances, even a small AVP-induced increase

in water flow might require a small depolymerization of actin. For example, 7.5 nM AVP produced only a slight increase in water flow across the bladder at 5 min, 10% of the maximal hydrosmotic response (4; unpublished data). Actin depolymerization, though significant, is 9% at this time point compared with a maximum depolymerization of 19% at 250 nM. Thus there was substantial depolymerization even at low water flows. In the $IMCD_2$ of the rat, we do not have as clear a picture of the physical relationship of the (presumed) vesicles carrying water channels to the actin network or to the apical membrane; nor do our studies establish as clearly as in the toad bladder the relationship between low AVP concentrations and low responses of water flow. We noted a 6% depolymerization of whole cell actin in the $IMCD_2$ at the lowest AVP concentration tested, 0.25 nM. The studies of Lankford et al. on the isolated perfused rat initial IMCD (14) showed a small increase in water flow when exposed to as little as 0.01 nM AVP for ≥10 min, and although the experimental protocols for the determination of water flow and actin depolymerization differed greatly, it is entirely possible that there is a fraction of water flow in the IMCD which responds to very low concentrations of AVP and does not require actin depolymerization. For example, a subpopulation of vesicles may be positioned so close to the apical membrane of the principal cell that fusion requires a minimum of translocation. Similar proposals have been made in studies of the isolated chromaffin cell, in which low levels of exocytosis may involve granules beyond the actin barrier and relatively close to the plasma membrane (2), and in the nerve terminal, where a "readily available" subpopulation of neurotransmitter vesicles is closely apposed to the plasma membrane, and a second "reserve pool" is the one requiring release from the cytoskeletal network (1, 11). It should also be noted that the aggrephores in the toad urinary bladder are very large structures, whereas the presumed vesicles carrying water channels in the mammalian kidney may very well have smaller diameters, making it easier for them to traverse the apical barrier. Nevertheless, they must be anchored in place in the unstimulated cell, as every organelle must be, and it is here that actin depolymerization may be critical in promoting fusion.

We thank I. Baptiste for excellent secretarial assistance.

This work was supported by National Institutes of Health Grants DK-03858 and CA-13330.

Present address of H. Simon: Dept. of Medicine, Kings County Hospital, 2094 Pitkin Ave., Brooklyn, NY 11207.

Address for reprint requests: R. M. Hays, Albert Einstein College of Medicine, Ullmann 617, 1300 Morris Park Ave., Bronx, NY 10461.

Received 2 February 1993; accepted in final form 14 April 1993.

REFERENCES

1. **Benfenati, F., F. Valkorta, and P. Greengard.** Computer modeling of synapsin I binding to synaptic vesicles and F-actin: implications for regulation of neurotransmitter release. *Proc. Natl. Acad. Sci. USA* 88: 575–579, 1991.
2. **Burgoyne, R. D.** Control of exocytosis in adrenal chromaffin cells. *Biochim. Biophys. Acta* 1071: 174–202, 1991.
3. **Condeelis, J., and A. L. Hall.** Measurement of actin polymerization and cross-linking in agonist-stimulated cells. *Methods Enzymol.* 196: 487–496, 1991.
4. **Ding, G., N. Franki, J. Condeelis, and R. M. Hays.** Vasopressin depolymerizes F-actin in the toad bladder epithelial cell. *Am. J. Physiol.* 260 (*Cell Physiol.* 29): C9–C16, 1991.
5. **Gao, Y., M. Cammer, N. Franki, H. Simon, H. Corey, M. Barac-Nieto, and R. M. Hays.** Confocal microscopy of thick sections of renal cortex and medulla (Abstract). *J. Am. Soc. Nephrol.* 3: 838, 1992.
6. **Gao, Y., N. Franki, F. Macaluso, and R. M. Hays.** Vasopressin decreases immunogold labeling of apical actin in the toad bladder granular cell. *Am. J. Physiol.* 263 (*Cell Physiol.* 32): C908–C912, 1992.
7. **Han, J.S., Y. Maeda, and M. A. Knepper.** High concentrations of vasopressin inhibit vasopressin-stimulated water transport in rat terminal IMCD (Abstract). *J. Am. Soc. Nephrol.* 3: 793, 1992.
8. **Hays, R. M., J. Condeelis, Y. Gao, H. Simon, G. Ding, and N. Franki.** The effect of vasopressin on the cytoskeleton of the epithelial cell. *Pediatr. Nephrol.* In press.
9. **Hays, R. M., N. Franki, and G. Ding.** Effects of antidiuretic hormone on the collecting duct. *Kidney Int.* 81: 530–537, 1987.
10. **Hays, R. M., and U. Lindberg.** Actin depolymerization in the cyclic AMP-stimulated toad bladder epithelial cell, determined by the DNase method. *FEBS Lett.* 280: 397–399, 1991.
11. **Hirokawa, N., K. Sobue, K. Kande, A. Harada, and H. Yorifugi.** The cytoskeletal architecture of the presynaptic terminal and molecular structure of synapsin 1. *J. Cell Biol.* 108: 111–126, 1989.
12. **Holmgren, K., K. E. Magnusson, N. Franki, and R. M. Hays.** ADH-induced depolymerization of F-actin in the toad bladder granular cell: a confocal microscope study. *Am. J. Physiol.* 262 (*Cell Physiol.* 31): C672–C677, 1992.
13. **Lacey, E. R.** Marked reduction in intramembranous particle clusters in the terminal portion of inner medullary collecting ducts of antidiuretic rats. *Cell Tissue Res.* 221: 583–595, 1982.
14. **Lankford, S. P., C.-L. Chou, Y. Terada, S. M. Wall, J. B. Wade, and M. A. Knepper.** Regulation of collecting duct water permeability independent of cAMP-mediated AVP response. *Am. J. Physiol.* 261 (*Renal Fluid Electrolyte Physiol.* 30): F554–F556, 1991.
15. **Madsen, K. M., W. L. Clapp, and J. W. Verlander.** Structure and function of the inner medullary collecting duct. *Kidney Int.* 34: 441–454, 1988.
16. **Sasaki, J., S. Tilles, J. Condeelis, J. Carbone, L. Meiteles, N. Franki, R. Bolon, C. Robertson, and R. M. Hays.** Electron-microscopic study of the apical region of the toad bladder epithelial cells. *Am. J. Physiol.* 247 (*Cell Physiol.* 16): C268–C281, 1984.
17. **Wall, S. M., J. S. Han, C.-L. Chou, and M. A. Knepper.** Kinetics of urea and water permeability activation by vasopressin in rat terminal IMCD. *Am. J. Physiol.* 262 (*Renal Fluid Electrolyte Physiol.* 31): F989–F998, 1992.
18. **Weigt, C., B. Schoepper, and A. Wegner.** Tropomyosin troponin complex stabilizes the pointed ends of actin filaments against polymerization and depolymerization. *FEBS Lett.* 260: 266–268, 1990.
19. **Zigmond, S. H., R. Furokawa, and M. Fechheimer.** Inhibition of actin filament depolymerization by the *Dictyostelium* 30,000-D actin-binding protein. *J. Cell Biol.* 119: 559–567, 1992.